

Heavy Ion Test Report for the AD9213 – 12 bit 10.0/6.0GSPS, JESD204B, ADC

Tom Decker

I. Introduction

The purpose of this test is to determine the heavy ion-induced single-event effects (SEE) susceptibility of the AD9213, a 12 bit, 10.0/6.0 GSPS, RF Analog-to-Digital Converter with 6.5 GHz input Bandwidth. The AD9213 features a 16-lane JESD204B interface, supporting its maximum bandwidth capability.

SEL susceptibility was evaluated at 10 GSPS, with no latch-up or other destructive SEE events observed to the highest LET tested of $\sim 85\text{MeV}\cdot\text{cm}^2/\text{mg}$ at a die temperature up to 121°C . Testing SEL at High temp is difficult due to the lid is critical for heat dissipation. Without a lid hot spots on the device will exceed the maximum junction temperature. Thermal characterizations have been performed on normal units as well as de-lidded units. A total of 3 devices have been tested with no evidence of SEL or any destructive effects. SEU, SEFI, and SET were also evaluated at sample rates of 6 GSPS and 10GSPS.

II. Device Under Test

The AD9213 is a 12-bit, 10.0/6.0 GSPS RF ADC designed to support communications applications capable of direct sampling wide bandwidth analog signals up to 5GHz. The AD9213 is based on an interleaved pipeline architecture with proprietary calibration and a randomization technique that suppressed interleaving spurious artifacts into its noise floor. The AD9213 operates at 10.0/6.0 GSPS and can be controlled through an SPI port. Figure 1 shows a functional block diagram of the device. Table I shows the device and test equipment details. AD9213 device parameters and functional descriptions can be found in the product datasheet.

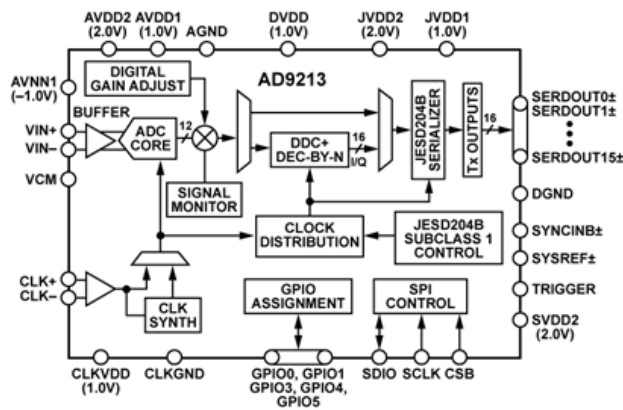


Figure 1. Schematic block diagram.

Table I

IV. Test Method

A. Test Setup

The devices under test (DUT) were de-lidded and the backside of the die was ground down such that the die was $\sim 50\mu\text{m}$ thick to ensure the ion beam would penetrate through the active area of the die. The AD9213 was configured using the ADS8-V1EBZ data capture board with a customized FPGA program to perform a Code Error Rate (CER) test. Figure 2 below shows the test setup. The AD9213 was powered up using the default register settings and a 10.0 GSPS clock was applied to the device for SEE tests. A coherent 700kHz sine wave was applied to the analog input and the data was captured by the ADS8-V1EBZ data capture board. A separate test was run monitoring 3 registers; for SEFI due to device resets. The DUT temperature was measured using internal diodes on the die. For SEL test, 5 Keithley triple power supplies were used to provide supply voltages to the DUT as well as monitor the supply currents.

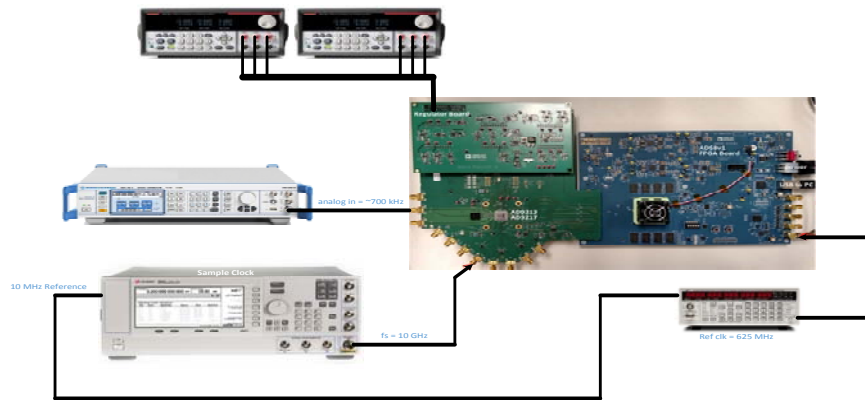


Figure 2. AD9213 data capture setup.

B. Irradiation procedure

A code error rate (CER) program was used to evaluate the SEFI/SET susceptibility. The code error rate program compared samples N and $N+1$, $N+1$ and $N+2$, etc, to a specified error threshold and captured specific data when the delta was over the error threshold. A custom Python script was used to control the testing.

The DUT was subjected to multiple ions with a flux ranging from $1.0 \text{ E}+3$ to $3.0 \text{ E}+3$. The script was setup to digitally reset the device when a SEFI, caused by a loss of the JESD204B link was detected. The power supplies were not cycled. During this test 3 additional registers were also monitored to detect a device reset condition which was recorded as SEFI.

The DUT was again subjected to various ion species with a flux ranging from $1.0 \text{ E}+2$ to $3.0 \text{ E}+3$. The number of individual bit upsets were recorded along with the quantity of device resets.

C. Test Conditions

Test Temperature:	Ambient temperature - air
Operating Frequency:	10.0/6.0 GHz
Power Supply(s):	1V, 2V
Angles of Incidence:	0°, 30°, 45°
Parameters:	CER - Output codes 10-Registers – SPI register reads SEL – Power Supply Current

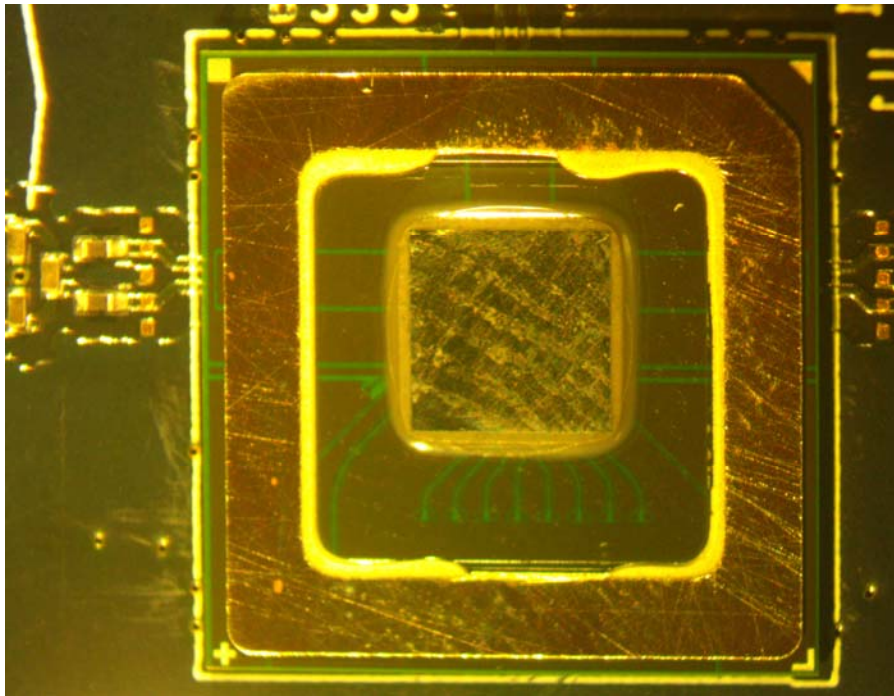


Figure 3. AD9213 with backside thinned to reduce the die thickness to <math><50\mu\text{m}</math>.

V. Results

Sample Clock = 10GSPS

SEL – No latch-up or destructive SEE events were observed on the AD9213 to the highest effective LET tested of ~ 87.2 MeV-cm²/mg. Angular dependence was evaluated at 101.5 MeV-cm²/mg with 30° angle. DUT die temperature, as measured using onboard diodes, was $\sim 121^\circ\text{C}$ for all SEL testing in Table A1 in the appendix. Table A2 shows 1 run on the device tested in April. Supply voltages were nominal and the effective LET was 77.3 MeV-cm²/mg. The sample tested in November was evaluated with different supply voltages and firmware due to the AD9213 was not released and the datasheet was not finalized. Data is not shown on the device tested in November to avoid confusion.

SEFI – Three devices have been tested at multiple LETs. Figure 4 shows the SEFI cross section for normal incident and 30° irradiation angles. The LET threshold is below an LET of 2.8 MeV-cm²/mg. The data plots are shown in the appendix. Die temperature was 90°C - 98°C. Data in June 2019 was taken with low supply voltages (-5%).

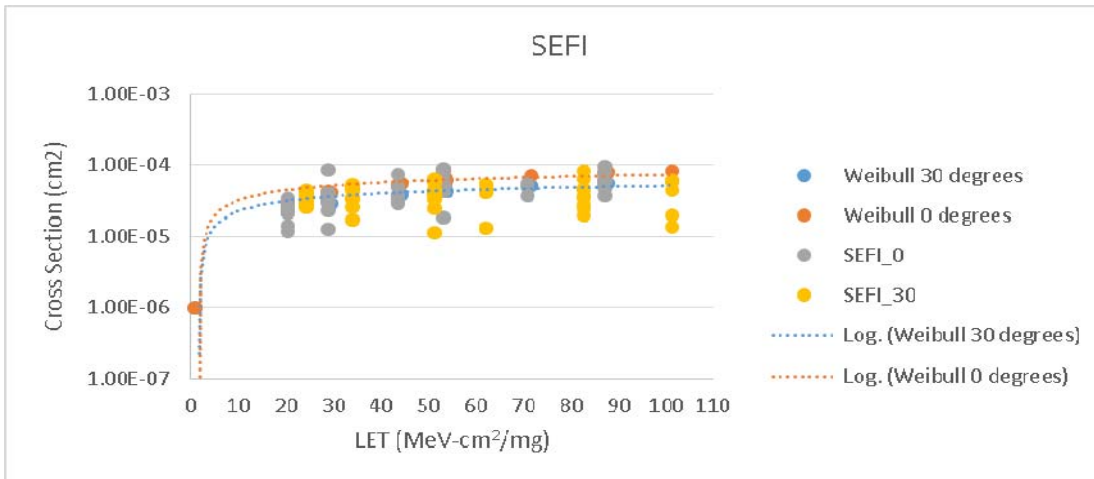


Figure 4: SEFI cross section vs. effective LET – June 2019

Weibull Parameters: 0°

LET_{th}: 1 MeV-cm²/mg S=1
Sigma = 1e-4 cm² W = 55 MeV-cm²/mg

Weibull Parameters: 30°

LET_{th}: 1 MeV-cm²/mg S=1
Sigma = 7e-5 cm² W = 55 MeV-cm²/mg

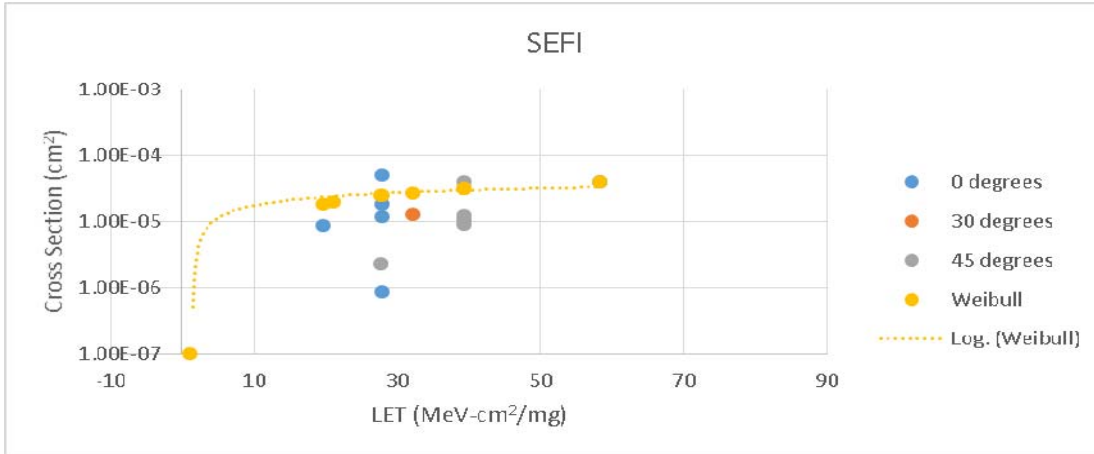


Figure 5: SEFI cross section vs. effective LET – April 2019

Weibull Parameters:

LET_{th}: 1 MeV-cm²/mg S=1
 Sigma = 6e-5 cm² W = 50 MeV-cm²/mg

SET - Multiple devices have been tested and sample SET plots are shown in the appendix. SET onset is <2.8MeV-cm²/mg. Weibull curves are shown below. The majority of the SET were DSET (Digital Transients).

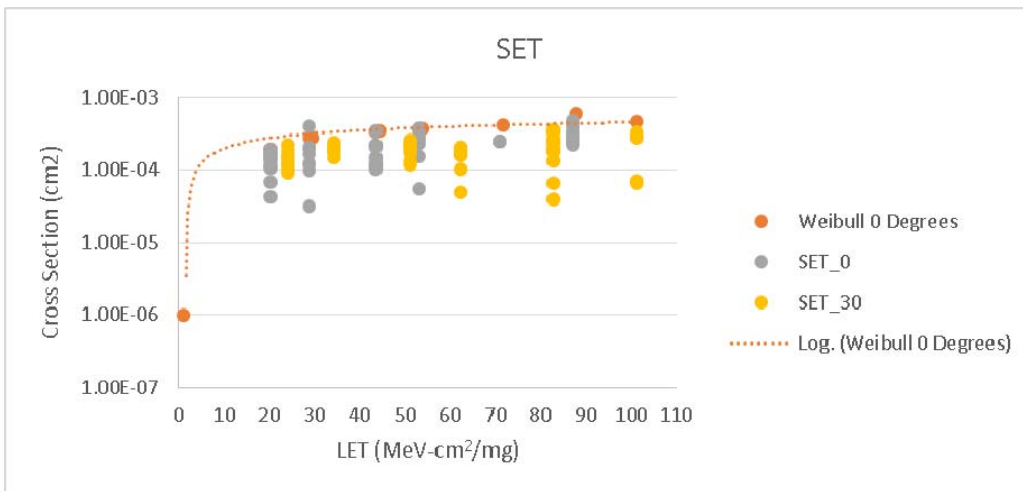


Figure 6: SET cross section for June 2019 – 2 samples

Weibull Parameters:

LET_{th}: 1 MeV-cm²/mg S = 0.7
 Sigma = 6e-4 cm² W = 55 MeV-cm²/mg

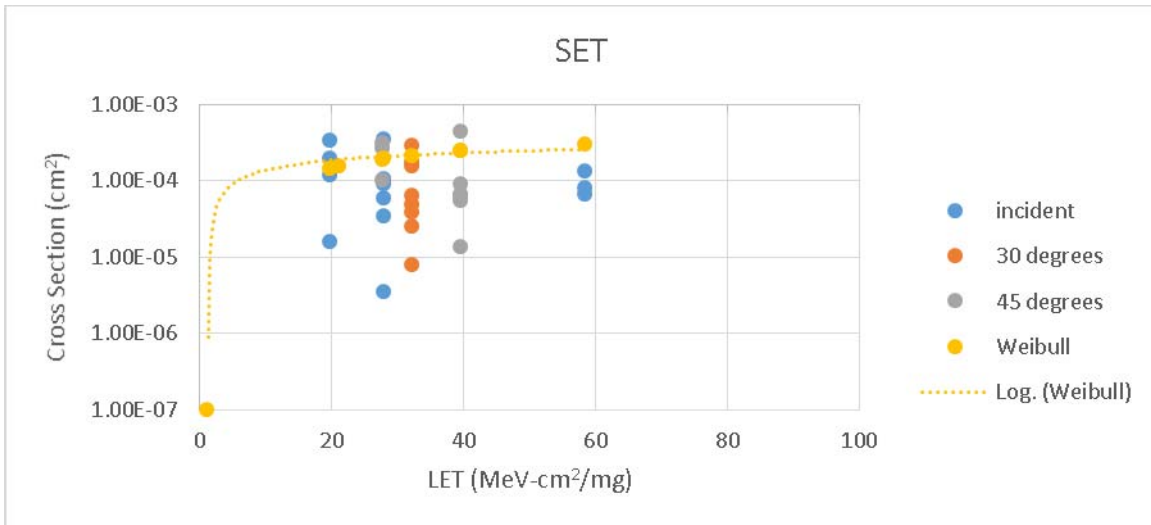


Figure 7: SET cross section for April 2019 – 2 samples

Weibull Parameters:

LET_{th}: 1 MeV-cm²/mg S = 1
 Sigma = 4e-4 cm² W = 40 MeV-cm²/mg

Sample clock: 6GSPS

SEL: One device was tested with a sample clock of 6GSPS at the internally monitored die temperature, ~90°C, with the flux set to 2.6e4 ions/s out to a fluence of 1e7 ions. The device did not suffer a destructive event at an effective LET of 85MeVcm²/mg.

SEFI: The device was characterized from 19.6 – 85.4 MeVcm²/mg. Results are shown in the appendix.

SET: Multiple device have been tested and sample SET plots are shown in the appendix. SET onset is <2.8MeV-cm²/mg.

Conclusion:

SEL: No evidence of SEL with high supply (Vs+5%) and at high temperature (121°C) ≤80MeV-cm²/mg.

SEFI: All SEFI are resettable through a soft reset (SPI). The dominant SEFI is the JESD204B link loss which is detectable by monitoring **SYNC BAR**. The threshold for SEFI is estimated to be 1 MeV-cm²/mg. Testing below 2.8MeV-cm²/mg was not performed. Apps note available.

SET: The majority of the SET are 1 clock cycle transients (DSET). The threshold for SET is estimated to be 1 MeV-cm²/mg. Testing below 2.8MeV-cm²/mg was not performed. ASETs are shown in the appendix with the longest being 513ns. Worst case transient went to +/-Full Scale.

Appendix

AD9213 Single Event Latch-Up Data Summary

		Angle	Energy	Eff LET	Eff Range	Flux	Fluence
Run	Ion	degrees	MeV	MeV-cm ² /mg	um	ions/cm ² /s	ions/cm ²
1	Au	0	1983	87.2	87.2	1.22E+03	3.21E+05
2	Au	0	1983	87.2	87.2	8.97E+02	7.48E+04
3	Au	0	1983	87.2	87.2	1.10E+03	3.06E+05
4	Au	0	1983	87.2	87.2	2.06E+03	5.74E+05
5	Au	0	1983	87.2	87.2	1.98E+03	2.79E+05
6	Au	0	1983	87.2	87.2	2.11E+03	2.59E+05
7	Au	0	1983	87.2	87.2	1.78E+03	1.28E+05
8	Au	0	1983	87.2	87.2	1.80E+03	1.74E+05
9	Au	30.1	1825	101.5	97.1	1.50E+03	7.08E+05
10	Au	30.1	1825	101.5	97.1	1.49E+03	3.56E+06
11	Au	30.1	1825	101.5	97.1	5.50E+03	9.38E+05

Table A1: SEL test run log June-2019 – 1 device

		Angle	Energy	Eff LET	Eff Range	Flux	Fluence
Run	Ion	degrees	MeV	MeV-cm ² /mg	um	ions/cm ² /s	ions/cm ²
51	TA	0	2076	77.3	118.6	8.96E+02	3.63E+05

Table A2: SEL test run log April-2019 – 1 device

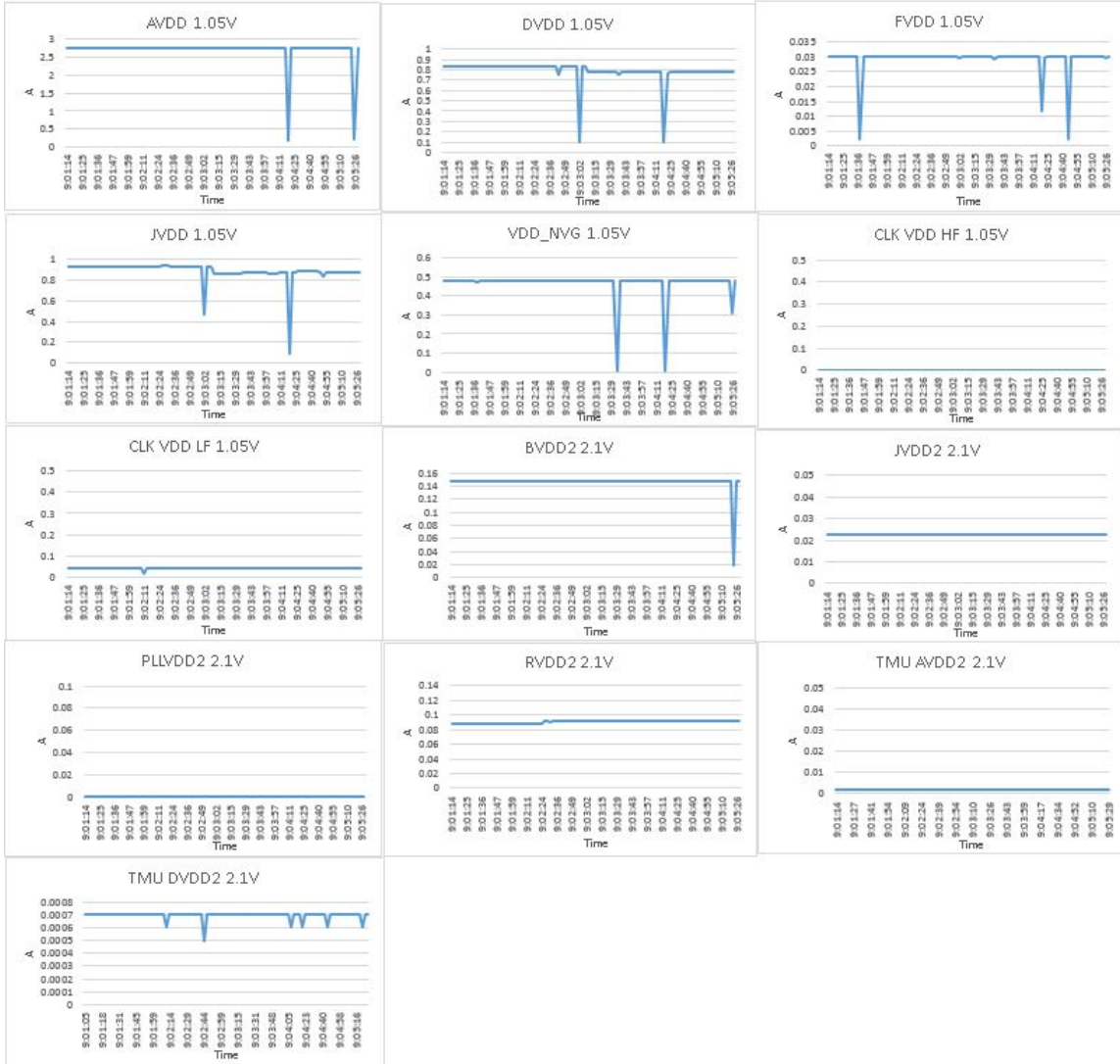


Figure A1: SEL Run 1 Power Supply Currents (Au - 87.2MeVcm²/mg)



Figure A2: SEL Run 2 Power Supply Currents (Au - 87.2MeVcm²/mg)

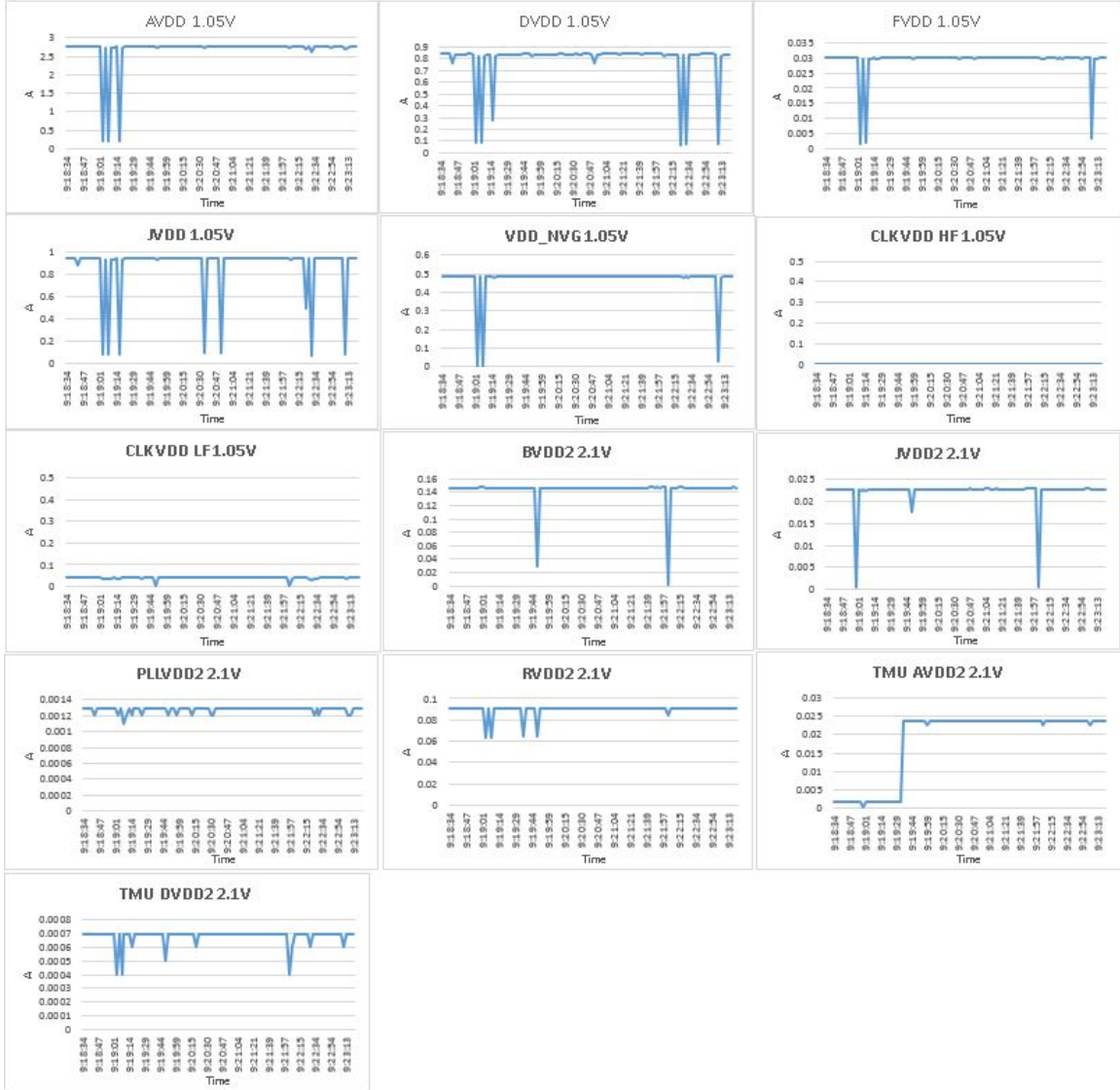


Figure A3: SEL Run 3 Power Supply Currents (Au - 87.2MeVcm²/mg)

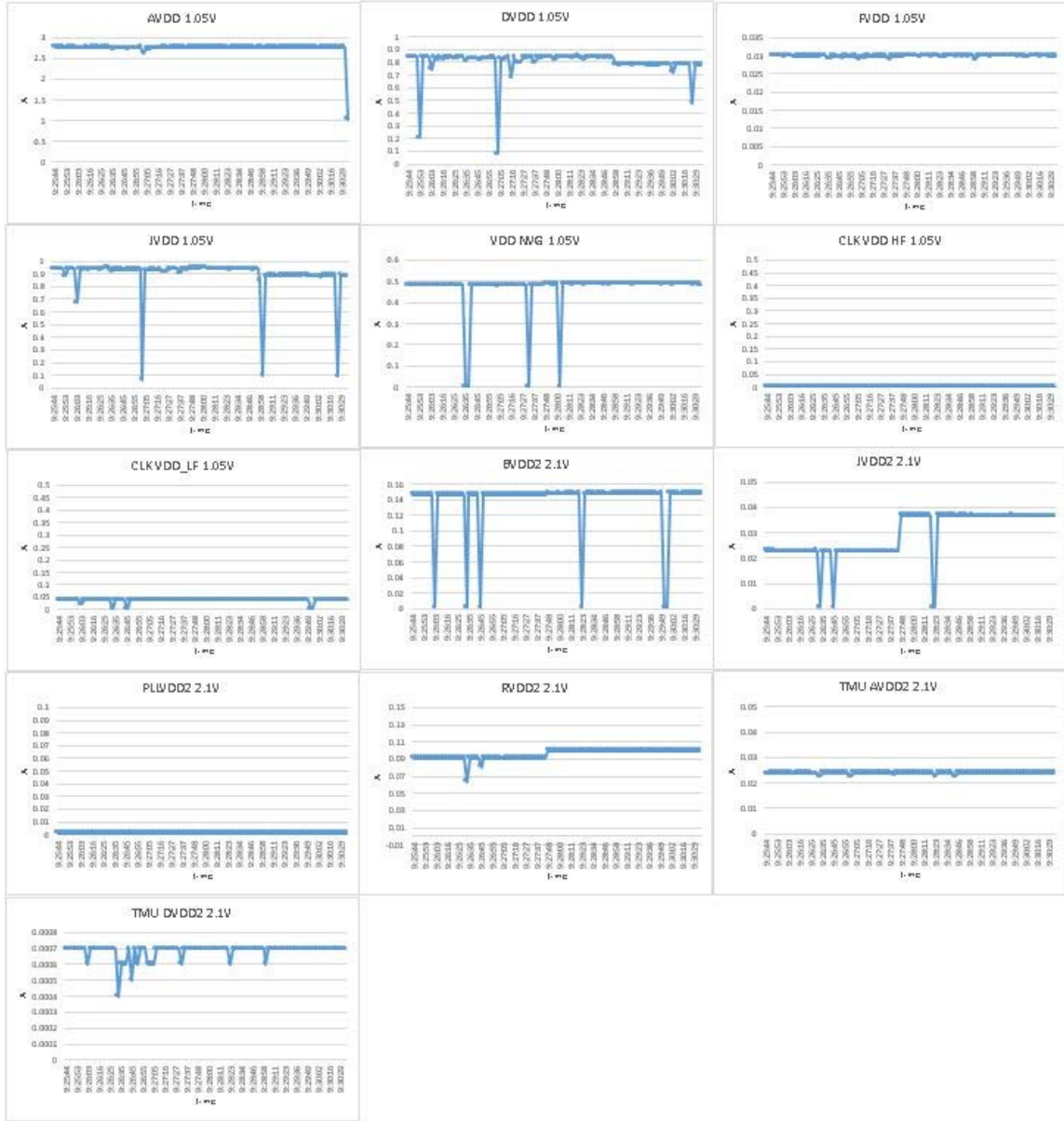


Figure A4: SEL Run 4 Power Supply Currents (Au - 87.2MeVcm²/mg)



Figure A5: SEL Run 5 Power Supply Currents (Au - 87.2MeVcm²/mg)

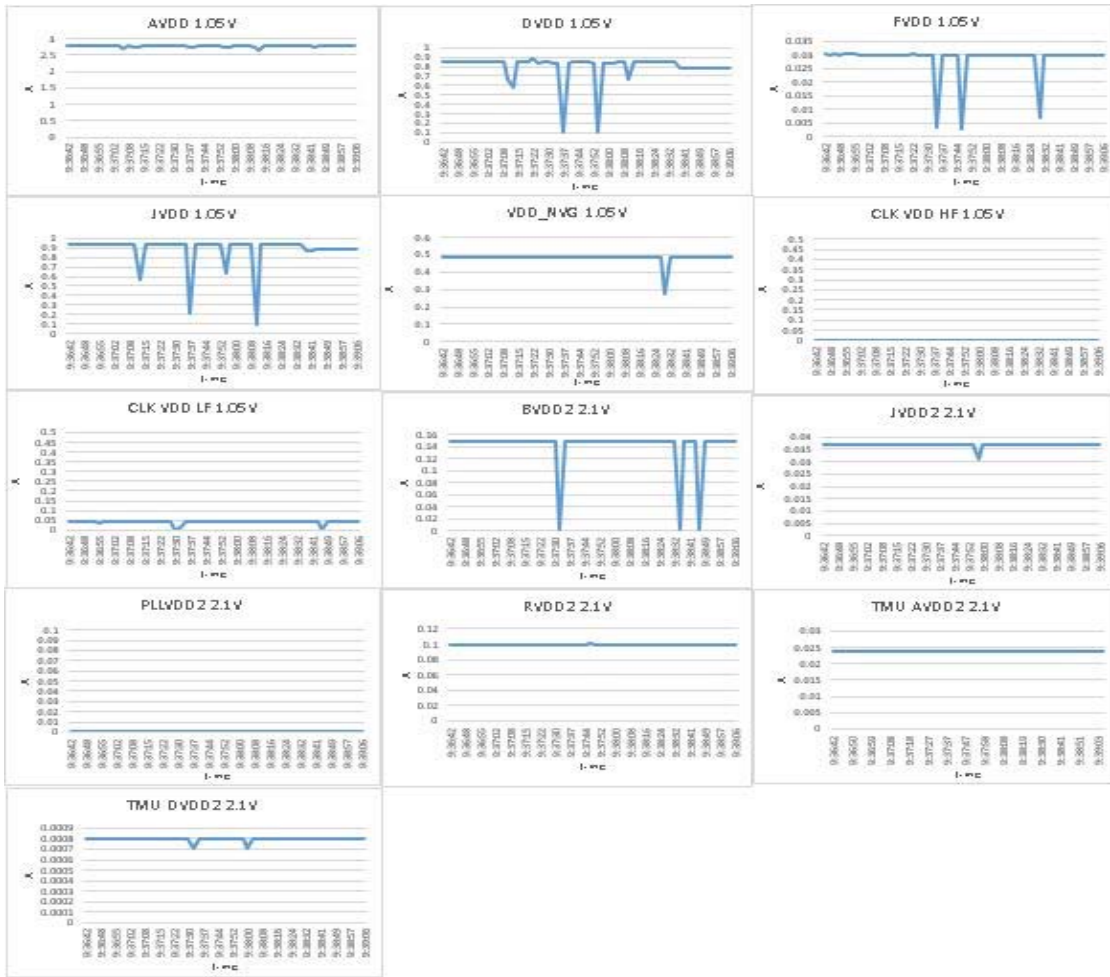


Figure A6: SEL Run 6 Power Supply Currents (Au - 87.2MeVcm²/mg)

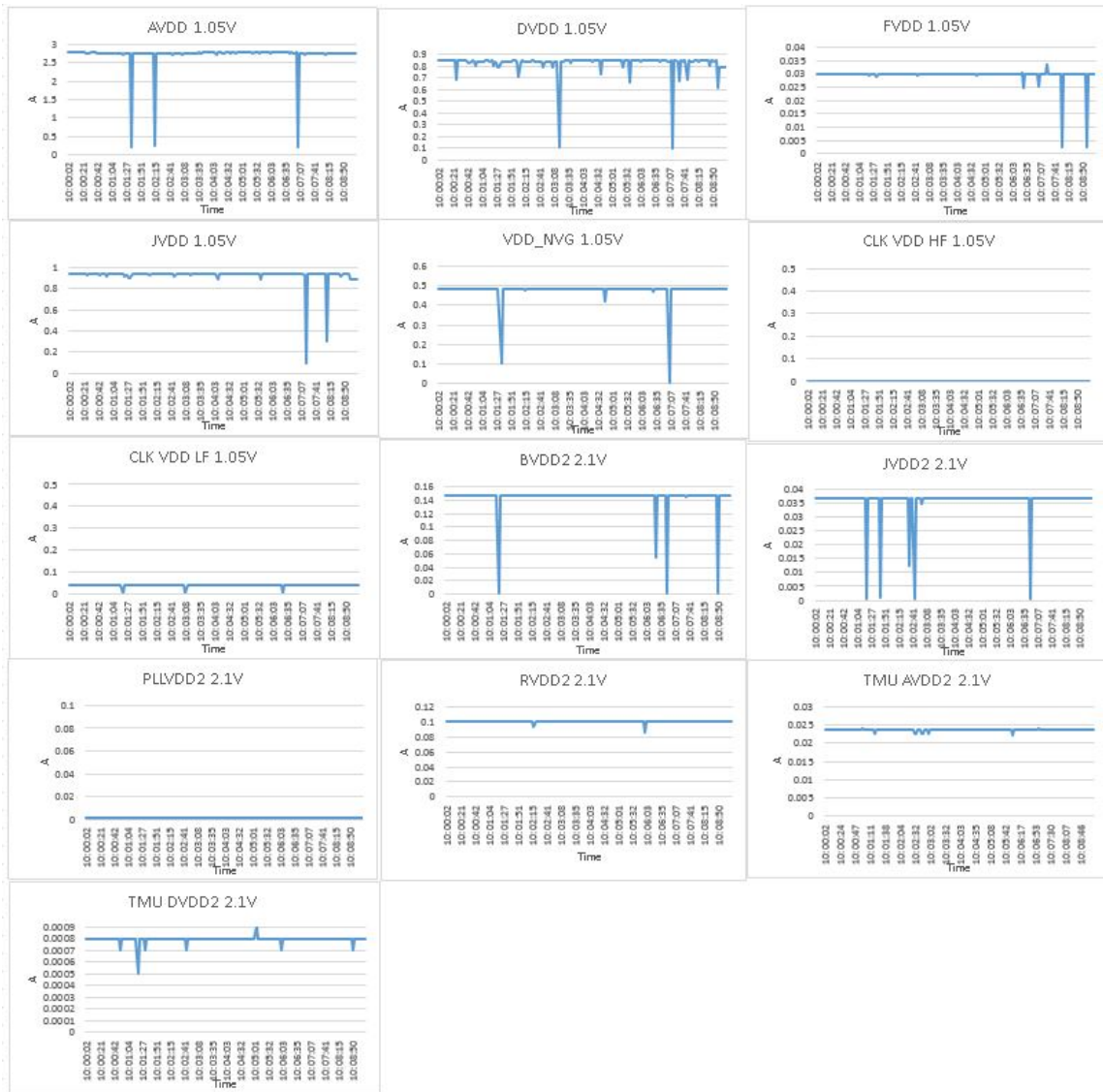


Figure A9: SEL Run 9 Power Supply Currents (Au (30°) – 101.5 MeVcm²/mg)

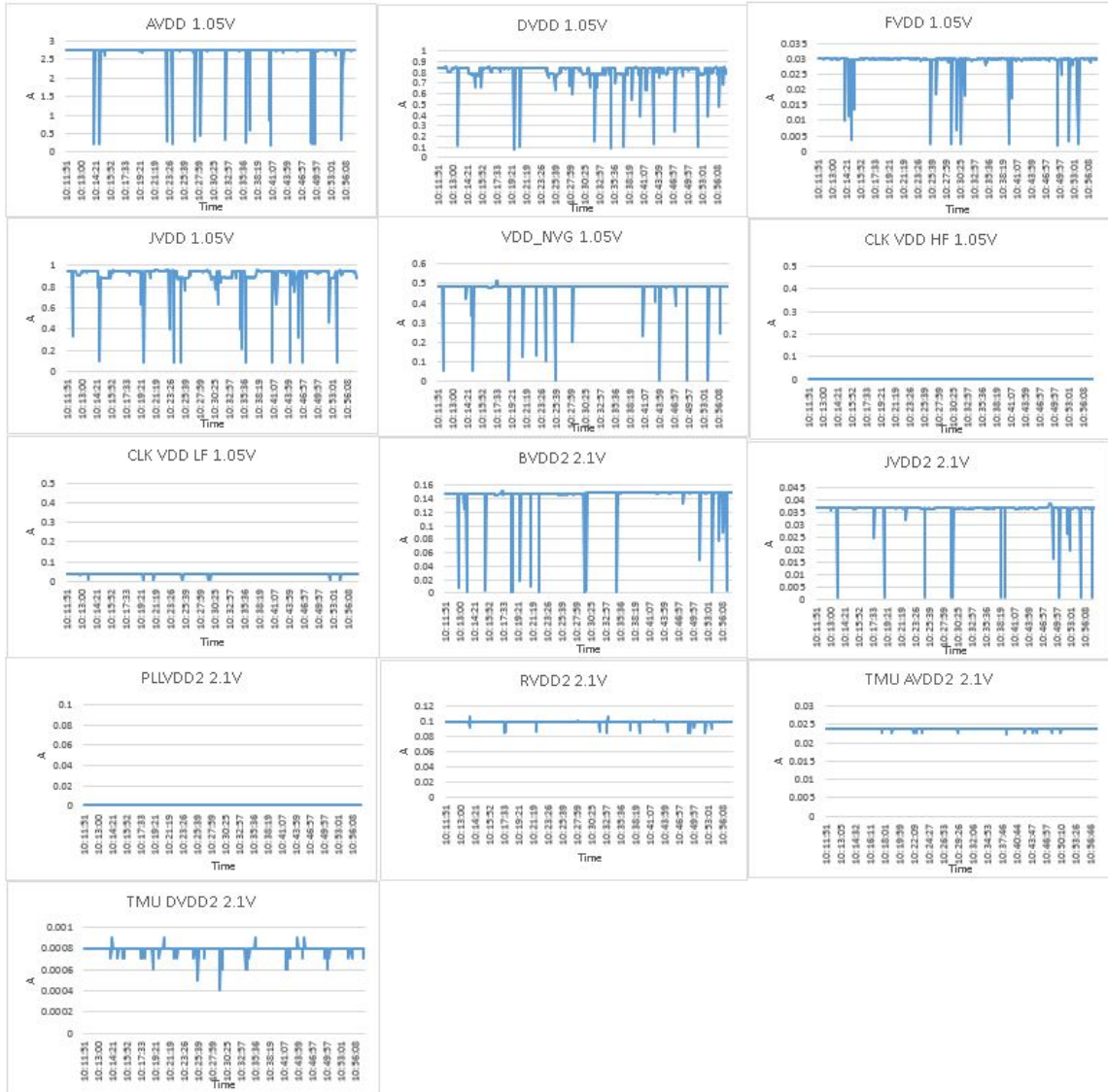


Figure A10: SEL Run 10 Power Supply Currents (Au (30°) – 101.5 MeVcm²/mg)

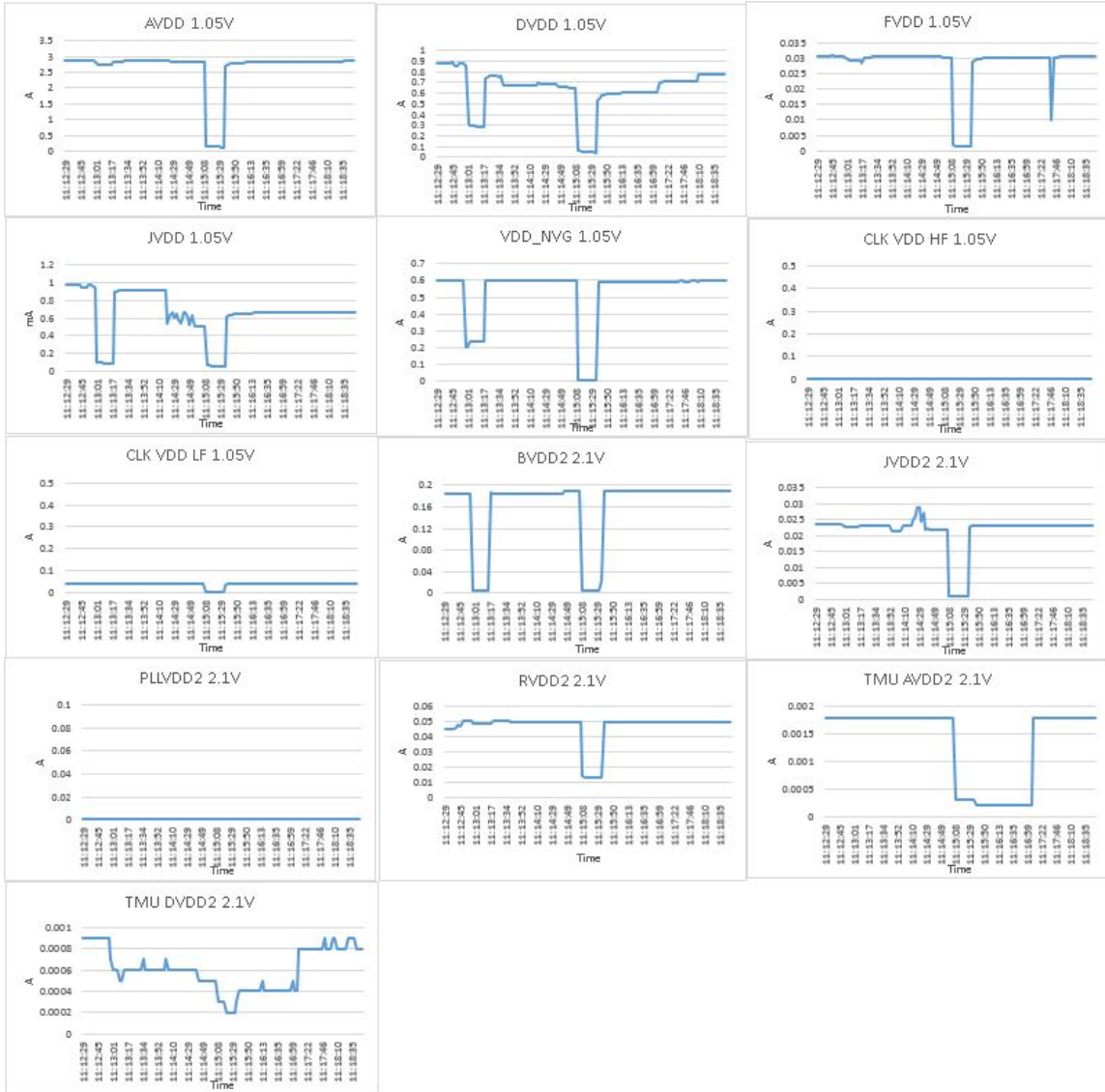


Figure A11: SEL Run 11 Power Supply Currents (Au (30°) – 101.5 MeVcm²/mg)



Figure A12: SEL Run 51 Power Supply Currents (Ta (0°) – 77.3 MeVcm²/mg) April 2019

AD9213 Single Event Transient Data Summary

The following plots illustrate the single event transient (SET) performance of the AD9213.

Two different types of SETs were observed. These are referred to as digital single event transient (DSET) and analog single event transient (ASET). A DSET is defined as an event where the ADC has a single sample delta that is beyond the error threshold. This SET is referred to as a DSET because typically a single sample error can be attributed to a digital error. An ASET is defined as an event where the ADC has multiple consecutive sample deltas that are beyond the error threshold or that exhibits an error behavior that lasts for multiple consecutive samples.

SET:

Run	Ion	Angle degrees	Eff LET MeV-cm ² /mg	Eff Range um	Flux ions/cm ² /s	Fluence ions/cm ²	SEFI # Events	SEFI CS cm ²	SET # Events	SET CS cm ²
1	Cu	0	20.4	122.3	1.00E+03	2.32E+04	0	0.00E+00	1	4.31E-05
2	Cu	0	20.4	122.3	1.00E+03	8.53E+04	1	1.17E-05	9	1.06E-04
3	Cu	0	20.4	122.3	2.86E+03	1.64E+05	4	2.45E-05	32	1.96E-04
9	Cu	0	20.4	122.3	1.42E+03	5.90E+04	2	3.39E-05	4	6.78E-05
10	Cu	0	20.4	122.3	1.26E+03	2.89E+05	6	2.08E-05	44	1.52E-04
11	Cu	0	20.4	122.3	1.76E+03	3.44E+05	8	2.32E-05	48	1.39E-04
12	Cu	0	20.4	122.3	1.20E+03	2.83E+05	6	2.12E-05	48	1.69E-04
13	Cu	0	20.4	122.3	1.31E+03	5.00E+05	7	1.40E-05	77	1.54E-04
14	Cu	0	20.4	122.3	1.36E+03	2.67E+05	7	2.63E-05	31	1.16E-04
15	Cu	0	20.4	122.3	1.45E+03	1.16E+05	3	2.58E-05	19	1.63E-04
16	Cu	30	24.2	105.9	2.15E+03	5.47E+05	17	3.11E-05	65	1.19E-04
17	Cu	30	24.2	105.9	2.05E+03	1.61E+05	6	3.74E-05	24	1.49E-04
18	Cu	30	24.2	105.9	2.19E+03	4.31E+05	12	2.79E-05	40	9.29E-05
19	Cu	30	24.2	105.9	2.30E+03	5.42E+05	24	4.43E-05	119	2.20E-04
21	Cu	30	24.2	105.9	2.17E+03	1.68E+05	5	2.99E-05	17	1.01E-04
22	Cu	30	24.2	105.9	2.23E+03	3.48E+05	9	2.59E-05	54	1.55E-04
23	Cu	30	24.2	105.9	2.23E+03	5.19E+05	13	2.51E-05	97	1.87E-04
24	Cu	30	24.2	105.9	2.20E+03	2.71E+05	11	4.07E-05	41	1.52E-04
25	Cu	30	24.2	105.9	2.17E+03	9.75E+05	32	3.28E-05	148	1.52E-04
26	Kr	30	34.2	97.7	3.30E+03	2.90E+05	5	1.72E-05	43	1.48E-04
27	Kr	30	34.2	97.7	3.24E+03	4.01E+05	10	2.50E-05	97	2.42E-04
28	Kr	30	34.2	97.7	3.35E+03	6.17E+05	30	4.87E-05	137	2.22E-04
29	kr	30	34.2	97.7	2.89E+03	3.90E+05	17	4.36E-05	73	1.87E-04
30	Kr	30	34.2	97.7	2.92E+03	3.82E+05	13	3.40E-05	88	2.30E-04
31	Kr	30	34.2	97.7	3.03E+03	5.05E+05	27	5.34E-05	112	2.22E-04
32	Kr	30	34.2	97.7	3.08E+03	3.04E+05	10	3.29E-05	54	1.78E-04
33	Kr	0	28.9	120.8	3.12E+03	4.30E+05	14	3.26E-05	82	1.91E-04
34	Kr	0	28.9	120.8	2.89E+03	1.61E+05	2	1.25E-05	5	3.12E-05
35	Kr	0	28.9	120.8	2.46E+03	3.13E+05	7	2.23E-05	64	2.04E-04
36	Kr	0	28.9	120.8	2.41E+03	5.51E+05	23	4.17E-05	92	1.67E-04
37	Kr	0	28.9	120.8	2.53E+03	2.24E+05	19	8.48E-05	143	6.38E-04
38	Kr	0	28.9	120.8	2.49E+03	4.65E+05	14	3.01E-05	94	2.02E-04
39	Kr	0	28.9	120.8	2.62E+03	7.41E+05	27	3.64E-05	129	1.74E-04
40	Kr	0	28.9	120.8	2.80E+03	6.29E+05	23	3.66E-05	109	1.73E-04
41	Ag	0	43.7	106.1	2.94E+03	4.85E+05	16	3.30E-05	66	1.36E-04
42	Ag	0	43.7	106.1	3.01E+03	2.66E+05	13	4.88E-05	68	2.55E-04
43	Ag	0	43.7	106.1	2.50E+03	1.67E+05	5	2.99E-05	25	1.50E-04
44	Ag	0	43.7	106.1	3.28E+03	4.27E+05	21	4.92E-05	89	2.09E-04
45	Ag	0	43.7	106.1	4.16E+03	2.66E+05	20	7.52E-05	105	3.95E-04
46	Ag	0	43.7	106.1	4.19E+03	4.02E+05	15	3.74E-05	59	1.47E-04
47	Ag	0	43.7	106.1	4.16E+03	2.51E+05	7	2.79E-05	26	1.04E-04
48	Ag	30	51.3	85.1	3.99E+03	3.91E+05	15	3.84E-05	94	2.41E-04
49	Ag	30	51.3	85.1	3.79E+03	3.54E+05	15	4.23E-05	85	2.40E-04
50	Ag	30	51.3	85.1	3.84E+03	3.94E+05	13	3.30E-05	88	2.23E-04
51	Ag	30	51.3	85.1	3.62E+03	1.77E+05	2	1.13E-05	21	1.19E-04
52	Ag	30	51.3	85.1	3.83E+03	9.30E+04	6	6.45E-05	16	1.72E-04
53	Ag	30	51.3	85.1	3.93E+03	3.37E+05	15	4.45E-05	74	2.20E-04
54	Ag	30	51.3	85.1	3.87E+03	3.39E+05	14	4.13E-05	76	2.24E-04
55	Ag	30	51.3	85.1	3.80E+03	3.92E+05	22	5.62E-05	113	2.89E-04
56	Ag	30	51.3	85.1	3.83E+03	2.01E+05	5	2.49E-05	27	1.34E-04

Table A3: SET test runs for June 16, 2019 – 1 sample

Run	Ion	Angle	Eff LET	Eff Range	Flux	Fluence	SEFI	SEFI CS	SET	SET CS		
		degrees	MeV-cm ² /mg	um	ions/cm ² /s	ions/cm ²	# Events	cm ²	# Events	cm ²		
17-Jun	11	Xe	0	53.2	106.6	1.61E+03	5.40E+04	1	1.85E-05	3	5.56E-05	
	12	Xe	0	53.2	106.6	1.37E+03	3.47E+05	29	8.36E-05	85	2.45E-04	
	13	Xe	0	53.2	106.6	1.15E+03	2.41E+05	13	5.40E-05	87	3.61E-04	
	14	Xe	0	53.2	106.6	9.47E+02	2.45E+05	22	8.97E-05	70	2.85E-04	
	15	Xe	0	53.2	106.6	8.29E+02	1.29E+05	8	6.22E-05	20	1.55E-04	
	16	Xe	0	53.2	106.6	7.00E+02	7.30E+04	6	8.22E-05	27	3.70E-04	
	17	Xe	0	53.2	106.6	1.42E+03	2.02E+05	10	4.94E-05	67	3.31E-04	
	18	Xe	0	53.2	106.6	1.28E+03	4.39E+05	19	4.33E-05	121	2.75E-04	
	19	Xe	0	53.2	106.6	1.06E+03	1.07E+05	9	8.41E-05	40	3.74E-04	
	20	Xe	0	53.2	106.6	8.68E+02	4.85E+05	28	5.78E-05	143	2.95E-04	
	21	Xe	30	62.3	85.5	2.95E+03	8.16E+04	0	0.00E+00	4	4.90E-05	
	22	Xe	30	62.3	85.5	2.64E+03	3.22E+05	14	4.34E-05	66	2.05E-04	
	23	Xe	30	62.3	85.5	2.67E+03	4.87E+05	26	5.34E-05	101	2.07E-04	
	24	Xe	30	62.3	85.5	2.65E+03	3.14E+05	15	4.78E-05	58	1.85E-04	
	25	Xe	30	62.3	85.5	2.43E+03	7.73E+04	1	1.29E-05	8	1.04E-04	
	26	Xe	30	62.3	85.5	2.10E+03	1.84E+05	8	4.35E-05	36	1.96E-04	
	27	Xe	30	62.3	85.5	2.24E+03	1.72E+05	8	4.66E-05	28	1.63E-04	
	28	Xe	30	62.3	85.5	2.14E+03	3.40E+05	14	4.12E-05	56	1.65E-04	
	29	Ho	30	82.8	85.4	2.50E+03	1.30E+05	6	4.63E-05	17	1.31E-04	
	30	Ho	30	82.8	85.4	2.55E+03	4.35E+05	16	3.67E-05	103	2.37E-04	
	31	Ho	30	82.8	85.4	2.70E+03	3.50E+05	16	4.58E-05	94	2.69E-04	
	32	Ho	30	82.8	85.4	2.83E+03	2.22E+05	10	4.51E-05	39	1.76E-04	
	33	Ho	30	82.8	85.4	3.02E+03	1.66E+05	4	2.42E-05	11	6.65E-05	
	34	Ho	30	82.8	85.4	2.04E+03	5.13E+04	1	1.95E-05	2	3.90E-05	
	35	Ho	30	82.8	85.4	2.04E+03	2.84E+05	18	6.33E-05	56	1.97E-04	
	36	Ho	30	82.8	85.4	1.92E+03	1.45E+05	12	8.26E-05	48	3.31E-04	
	37	Ho	30	82.8	85.4	1.99E+03	7.29E+04	2	2.74E-05	26	3.57E-04	
	38	Ho	30	82.8	85.4	2.02E+03	1.16E+05	4	3.45E-05	40	3.45E-04	
	39	Ho	0	71	106.4	2.14E+03	3.21E+05	16	4.98E-05	81	2.52E-04	
	40	Ho	0	71	106.4	2.17E+03	2.88E+05	16	5.55E-05	72	2.50E-04	
	41	Ho	0	71	106.4	2.08E+03	2.75E+05	10	3.64E-05	69	2.51E-04	
	18-Jun	1	Au	0	87.2	104.9	1.42E+03	4.47E+05	34	7.61E-05	225	5.04E-04
		2	Au	0	87.2	104.9	1.10E+03	3.23E+05	21	6.5E-05	120	3.71E-04
		3	Au	0	87.2	104.9	9.44E+02	2.51E+05	24	9.581E-05	139	5.55E-04
		4	Au	0	87.2	104.9	2.48E+03	2.96E+05	11	3.721E-05	74	2.50E-04
		5	Au	0	87.2	104.9	2.51E+03	2.70E+05	13	4.811E-05	60	2.22E-04
		6	Au	0	87.2	104.9	2.61E+03	4.07E+05	24	5.892E-05	104	2.55E-04
		7	Au	0	87.2	104.9	1.68E+03	1.81E+05	10	5.534E-05	73	4.04E-04
		8	Au	0	87.2	104.9	2.31E+03	2.20E+05	12	5.452E-05	62	2.82E-04
		9	Au	0	87.2	104.9	2.33E+03	4.40E+05	24	5.46E-05	123	2.80E-04
		10	Au	0	87.2	104.9	2.01E+03	4.97E+05	26	5.232E-05	174	3.50E-04
11		Au	30	101.3	84.2	2.61E+03	5.87E+05	26	4.429E-05	167	2.84E-04	
12		Au	30	101.3	84.2	2.61E+03	2.93E+05	17	5.81E-05	82	2.80E-04	
14		Au	30	101.3	84.2	2.42E+03	3.60E+05	22	6.108E-05	105	1.80E-01	
16	Au	30	101.3	84.2	2.91E+03	2.24E+05	3	1.339E-05	15	6.70E-05		
17	Au	30	101.3	84.2	2.56E+03	3.52E+05	21	5.966E-05	116	2.03E-01		
18	Au	30	101.3	84.2	2.14E+03	8.36E+04	0	0	6	4.43E-02		
21	Au	30	101.3	84.2	1.91E+03	1.04E+05	2	1.931E-05	7	6.76E-05		

Table A4: SET runs for June 17 & 18, 2019 – 1 sample

Run	Dut	Ion	Angle	LET (Mevcm ² /mg)	Flux (ions/s)	Fluence (ions)	SEFI	SEFI Cross Section	SET	SET Cross Section
7	1	Cu	0.197	19.6	9.64E+02	1.85E+05	0		3	1.62E-05
10	1	Cu	0.197	19.6	1.01E+03	2.99E+05	0		101	3.38E-04
11	1	Cu	0.197	19.6	1.03E+03	1.20E+05	0		24	2.00E-04
12	1	Cu	0.197	19.6	8.98E+02	1.15E+05	1	8.7E-06	14	1.22E-04
13	1	Cu	45	27.7	1.04E+03	8.87E+04	0		9	1.01E-04
14	1	Cu	45	27.7	1.00E+03	9.43E+04	0		30	3.18E-04
15	1	Cu	45	27.7	9.52E+02	1.62E+04	0		0	
16	1	Cu	45	27.7	9.88E+02	4.18E+05	1	2.39E-06	111	2.66E-04
19	1	Kr	45	39.4	1.20E+03	1.61E+05	2	1.24E-05	72	4.46E-04
20	1	Kr	45	39.4	1.13E+03	9.25E+04	1	1.08E-05	0	
21	1	Kr	45	39.4	1.10E+03	2.33E+05	0		15	6.43E-05
22	1	Kr	45	39.4	1.06E+03	8.28E+04	0		5	6.04E-05
23	1	Kr	45	39.4	1.07E+03	1.29E+05	0		12	9.31E-05
24	1	Kr	30	32.1	9.41E+02	7.62E+04	1	1.31E-05	22	2.89E-04
25	1	Kr	30	32.1	9.30E+02	6.33E+04	0		10	1.58E-04
26	1	Kr	30	32.1	9.03E+02	5.60E+04	0		10	1.79E-04
27	1	Kr	30	32.1	8.22E+02	7.98E+04	0		4	5.02E-05
28	1	Kr	0	27.8	8.01E+02	1.30E+05	0		13	1.00E-04
29	1	Kr	0	27.8	5.73E+02	8.93E+04	0		32	3.58E-04
30	1	Kr	0	27.8	8.70E+02	1.44E+05	0		5	3.48E-05
31	2	Kr	0	27.8	1.02E+03	8.27E+04	1	1.21E-05	9	1.09E-04
32	2	Kr	0	27.8	1.08E+03	2.74E+05	14	5.11E-05	25	9.12E-05
33	2	Kr	0	27.8	1.07E+04	1.13E+06	1	8.86E-07	4	3.54E-06
34	2	Kr	0	27.8	2.28E+03	4.96E+05	9	1.81E-05	30	6.05E-05
35	2	Kr	30	32.1	2.12E+03	1.25E+05	0		1	7.99E-06
36	2	Kr	30	32.1	2.20E+03	2.34E+05	6	2.57E-05	6	2.57E-05
37	2	Kr	30	32.1	2.20E+03	2.57E+05	2	7.77E-06	10	3.89E-05
38	2	Kr	30	32.1	2.08E+03	1.83E+05	2	1.09E-05	12	6.54E-05
39	2	Kr	45	39.4	2.01E+03	2.19E+05	2	9.14E-06	12	5.49E-05
40	2	Kr	45	39.4	1.92E+03	7.28E+04	0		1	1.37E-05
41	2	Kr	45	39.4	1.88E+03	2.52E+05	10	3.97E-05	17	6.74E-05
43	2	Pr	0	58.3	1.88E+03	1.47E+05	6	4.09E-05	20	1.36E-04
44	2	Pr	0	58.3	2.24E+03	9.85E+04	0		8	8.12E-05
45	2	Pr	0	58.3	9.77E+02	2.93E+04	0		2	6.82E-05

Table A5: SET runs for April 2019 – 2 samples

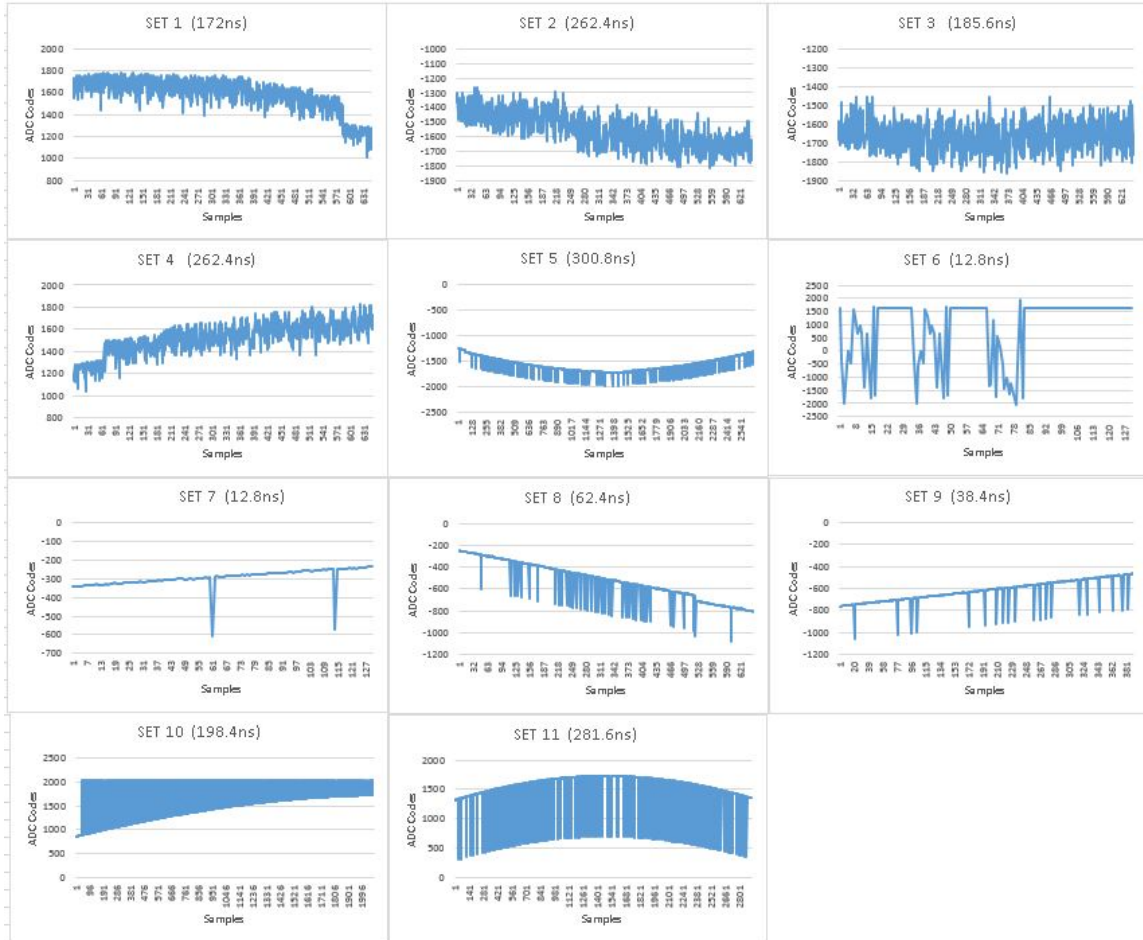


Figure A13: Sample SET plots for 10GSPS @ effective LET of 101MeVcm²/mg (June 2019)

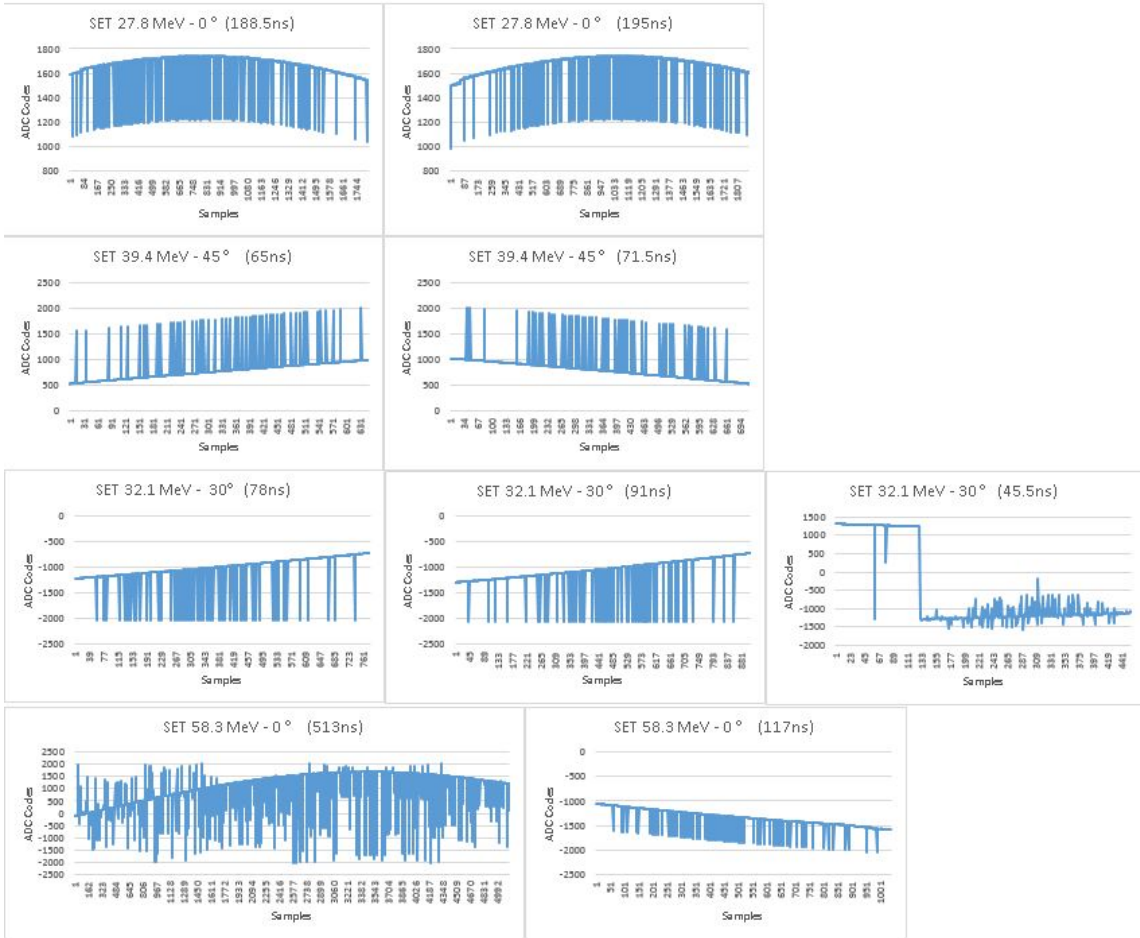


Figure A14: Sample SET plots from April 2019

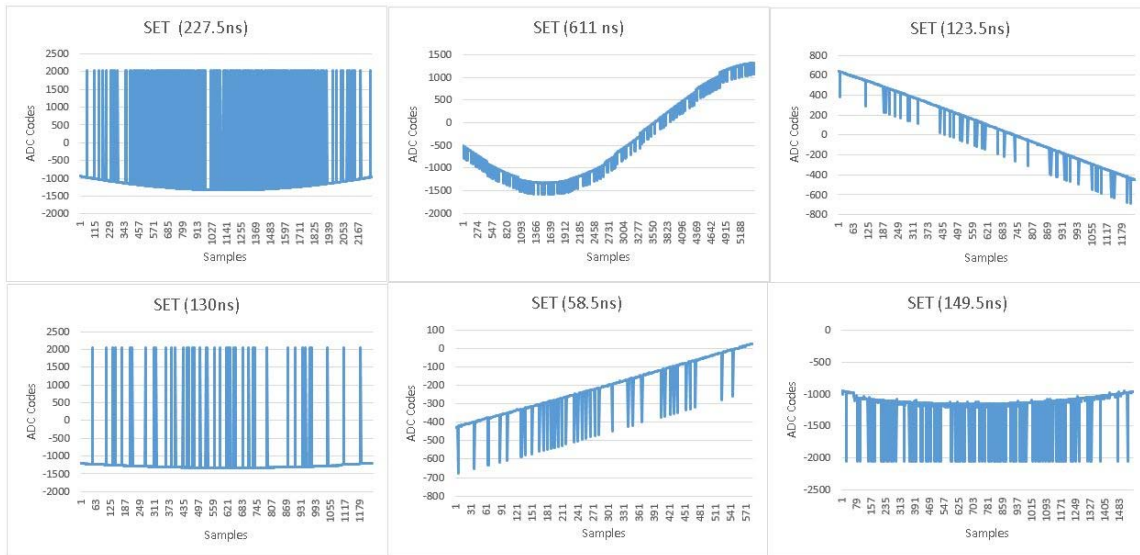


Figure A15: Sample SET plots from November 2018 @ effective LET of 85.4MeV-cm²/mg – 6GSPS